

Rheology of concentrated suspensions containing mixtures of spheres and fibres

Journal Article**Author(s):**

Marti, Irene; Höfler, Oliver; Fischer, Peter; Windhab, Erich J.

Publication date:

2005-07

Permanent link:

<https://doi.org/10.3929/ethz-b-000032815>

Rights / license:

[In Copyright - Non-Commercial Use Permitted](#)

Originally published in:

Rheologica Acta 44(5), <https://doi.org/10.1007/s00397-005-0432-9>

Irene Marti
Oliver Höfler
Peter Fischer
Erich J. Windhab

Rheology of concentrated suspensions containing mixtures of spheres and fibres

Received: 8 December 2004
Accepted: 9 December 2004
Published online: 12 March 2005
© Springer-Verlag 2005

Originally presented at the Annual European Rheology Conference 2003, AERC 2003

I. Marti · O. Höfler · P. Fischer (✉)
E. J. Windhab
Laboratory of Food Process Engineering,
ETH Zentrum, ETH Zürich,
Institute of Food Science and Nutrition,
8092 Zürich, Switzerland
E-mail: peter.fischer@ilw.agrl.ethz.ch
Tel.: +41-1-6325349
Fax: +41-1-6321155

Abstract Optimising flow properties of concentrated suspensions is an important issue common for many industries. The rheology of concentrated suspensions has therefore been studied intensively both experimentally and theoretically. Most studies have focused on monodisperse and polydisperse suspensions of either spheres or fibres. In practice, most suspensions contain particles that are polydisperse both in size and shape. A mixing rule for such systems is expected to be a powerful tool for engineers and product designers. Therefore in this work, suspensions of spheres, fibres and mixtures thereof were characterised using

rotational shear rheometry and in-line image analyses. Thereby, total solids volume concentration and fibre fraction was varied. Results from transient and steady-state shear rheometry are discussed with respect to concentration, fibre fraction, and shear induced microstructure. Experimentally obtained viscosity data were accurately fitted using the model proposed by Farris (T Soc Rheol 12:281, 1968) for mixtures of monodisperse non-interacting spheres of different sizes.

Keywords Sphere/fibre suspensions · Mixing rules · Shape polydispersity

Introduction

Non-colloidal concentrated suspensions are frequently encountered in industrial process unit operations like pumping, mixing and transportation. Concrete, ceramics, composites, paint, and food products are some examples for industrial applications. From the processing side, it is important to predict the rheological properties of suspension systems as a function of various physical and chemical properties of the suspended particles and the fluid as well. A clear goal for a food designer is, e.g. to produce low calorie, high solid content confectionery products, such as chocolates or nut pastes, with the same perceived textural properties as the full fat product. To tackle this problem, improved particle packing performance with reduced liquid phase volume is an economically high potential

alternative to fat substitution by other fluids (Villagran et al. 1996).

In recent decades, progress in theoretical description and experimental measurements was made for concentrated suspensions containing monodisperse and polydisperse particles. Suspensions containing monodisperse spherical particles at high concentrations were studied intensively by various authors (Mooney 1951; Krieger and Dougherty 1959; Frankel and Acrivos 1967; Frith et al. 1987; Buscall 1991; Schmidt and Münstedt 2002). A number of studies focussed on concentrated bidisperse and polydisperse suspensions of spheres, and progress was reported (Farris 1968; Sudduth 1993; Chang and Powell 1994; Probst et al. 1994; Gonderet and Petit 1997; Qin and Zaman 2003). Some experimental work was done to investigate the effect of particle properties on the rheology of concentrated polydisperse

suspensions (Dabak and Yucel 1986; Tsai et al. 1992). Time-dependent rheology of concentrated suspensions is covered in the literature by concise reviews of Mewis (1979) and Barnes (1989, 1997). Theories of fibre suspension rheology were recently reviewed by Petrie (1999). The description of fibre orientation in flow is the main objective of experimental studies carried out with concentrated fibre suspensions (Stover et al. 1999; Barbosa et al. 1994). Experimental work treating the effect of fibre orientation on the rheology can also be found (Ganani and Powell 1985; Petrich et al. 2000). However, most suspensions encountered in practice are polydisperse, not only in size but also in shape. For the time being, a systematic investigation devoted to the problem of shape polydispersity cannot be found in the literature.

It is well established that the viscosity of suspensions increases as the solids volume concentration, c_v , increases (Mewis and Macosco 1993). The qualitative characteristics of the viscosity versus shear rate curves resemble the ones of the continuous phase at low-volume fractions of about 1%. Increase in concentration leads to the occurrence of shear thinning at intermediate shear rates. At further increase of concentration, an apparent yield stress in the low shear rate regime becomes evident. And at very high concentrations, approaching the maximum packing fraction, shear thickening can occur at high shear rates.

As the solids volume concentration is increased, suspended particles begin to interact, and the viscosity increases more than linearly with volume concentration. Interaction effects can be accounted for by a power series expansion of the Einstein equation (Einstein 1906):

$$\eta = \eta_s(1 + k_E c_v) \quad (1)$$

where η is the viscosity of the suspension, η_s is the viscosity of the continuous phase, c_v is the solids volume concentration, and k_E is the Einstein coefficient, which equals 2.5 for non-interacting particles of spherical shape. Since higher order coefficients are difficult to calculate, semiempirical models are usually used for the description of concentrated suspensions. The volume fraction dependence of the low and high shear rate limiting relative viscosities, η_r , is well described by the Krieger–Dougherty equation (Krieger 1972), see Eq. 2

$$\eta_r = \frac{\eta}{\eta_s} = \left(1 + \frac{c_v}{c_{v,\max}}\right)^{-k c_{v,\max}} \quad (2)$$

where k is a shape factor, and equals k_E in Eq. 1. The maximum packing fraction, $c_{v,\max}$, depends on the physical characteristics of the particles, the particle size distribution, and the suspension structure.

Possibly, the most important factor affecting the maximum packing fraction of highly concentrated sus-

pensions is the particle size distribution. Because smaller particles can fit into the voids of bigger ones, the maximum packing fraction increases gradually from monodispersed particle systems to polydispersed particle systems.

Two different approaches are used in the development of predictive methods treating the problem of size distribution. In the effective volume fraction approach, the maximum packing fraction is typically expressed as a function of particle size ratio, fraction of coarse particles, and particle orientation factors (Windhab 2000). Derived equations have generally the form of Eq. 2. The second class is based on the separation of contribution parameters. Thereby, the contribution from parameters, such as fine particles and coarse particles, are considered individually. The suspension viscosity is expressed as a combination of these parameters.

Farris (1968) was one of the first investigators to define the relative viscosity as the contributions from fine and coarse particles separately. According to his model, see Eq. 3, a bimodal system can be represented as a coarse fraction suspended in a matrix of fine particles with the two fractions behaving independently of each other. To calculate the relative suspension viscosity, he assembled viscosity data of monodispersed distributions.

$$\eta_r = \frac{\eta}{\eta_s} = \left(\frac{\eta_f}{\eta_s}\right) \left(\frac{\eta}{\eta_f}\right) = \eta_{fr} \eta_{cr} = H(c_{v,f}) H(c_{v,c}) \quad (3)$$

where η_{fr} is the relative viscosity of fines and is defined as the ratio of the viscosity of the suspensions containing just the fine particles, η_f , to the viscosity of the suspending fluid, η_s . The relative viscosity of the coarse fraction, η_{cr} , is the contribution from the coarse particles. It is defined as the ratio of the viscosity of the suspension, η , to the viscosity of the fine fraction, η_f . H is the functional of corresponding variables. The volume fraction of the fine particles, before adding the coarse particles to the suspension, and the volume fraction of coarse particles are labelled $c_{v,f}$ and $c_{v,c}$, respectively. For non-colloidal suspensions with non-interacting spherical particles, and where the size ratio of the suspended particles is greater than 10, excellent agreement between experiment and Farris model can be found (Qin and Zaman 2003). The maximum packing fraction of concentrated suspensions is very sensitive to the properties of suspended particles and is controlled by the type of particle packing. When particles have irregular shapes, particle packing efficiency is expected to differ from the case of spheres, and thus suspension viscosity is affected.

In principle anisotropic particles such as fibres, could be packed more tightly than spheres, although they would start to interact at lower concentrations. In reality, higher viscosities are normally found with anisotropic particles. The concentration dependency is

approximately exponential at low to moderate concentrations, but still can be modelled using equations similar to Eq. 2. For suspensions of fibres, the empirical value of $c_{v, \max}$ was found to decrease roughly linear with increasing fibre aspect ratio (Metzner 1985). Furthermore due to hydrodynamic forces, anisotropic particles tend to align in the direction of flow. The packing density of such particle systems becomes, therefore, also a function of shear history (Barnes 1989; Windhab 2000).

The intention of this study is to characterise the influence of the total volume concentration and the fibre fractions in the disperse phase on the flow behaviour of suspensions made up with mixtures of spheres and fibres. Rotational shear rheometry was used to investigate the transient effect of shear deformation at constant applied shear rate as well as the effect of shear rate on the viscous behaviour of the suspensions. In addition to the rheological characterisation, in-line image analysis was used as a tool to study the evolution of fibre angle distribution as a function of applied shear treatment. It will be shown that for the studied suspensions systems the orientation behaviour of the fibres is not affected by the fibre fraction. Fibre angle distribution is rather a function of shear history than a function of applied shear rate. To conclude, an attempt is made to model the viscous behaviour of the treated suspension systems. It will be demonstrated that the high shear rate relative viscosities of suspensions made up with mixtures of spheres and fibres can be accurately fitted using the Farris model.

Experimental

Materials

Silicon oils (polydimethylsiloxanes) AK2000 and AK5000 obtained from Wacker-Chemie GmbH with a density of $\rho_{25\text{ }^\circ\text{C}} = 0.97\text{ g cm}^{-3}$ and a zero shear viscosity of $\eta_{25\text{ }^\circ\text{C}} = 1.94\text{ Pa s}$ and 5.01 Pa s , respectively were chosen as the suspending fluids. The used oils exhibit Newtonian flow behaviour up to a shear rate of around $1,000\text{ s}^{-1}$. The suspending fluid was chosen in such a manner that no sedimentation occurred on the time scale of the longest measurements.

Hollow glass spheres from Potters Europe (Spherical CP00) with a density of 1.1 g cm^{-3} and glass fibres from Vetrotex International (1304) with a density of 2.6 g cm^{-3} were used as filler particles. The fibre diameter was chosen to correspond with the diameter of the spheres. Distributions of fibre diameter and length were obtained using image analysis, whereas a minimum of 1,000 measurements was assembled to calculate the distribution parameters. Micrographs were taken using an inverse light microscope (Diaphot-TMD, Nikon AG)

equipped with a 10 \times and a 20 \times objective, for fibre diameter measurements and fibre length measurements, respectively. Images were grabbed with a CCD-camera (3Cck Color Video Camera KY-F55B, JVC) on a Macintosh computer using a Quick Capture frame grabber card from Data Translation. Image grabbing and ensuing image analysis were performed using the public domain software NIH Image. The laser diffraction instrument Malvern Mastersizer-X was used to measure particle size distributions of the hollow glass spheres. The sample material was dispersed into deionised water using an ultrasound dispersing device (T480/H-2, Elma). The dispersions were further diluted to a laser beam obscuration of 15–20%. Average size distribution parameters of the physical dimensions of the glass filler particles are represented in Table 1. The average fibre aspect ratio results in 7.64.

Sample preparation

In order to reduce effects of adsorbed water on the surface of the hydrophilic filler particles, they were dried in a vacuum oven at $130\text{ }^\circ\text{C}$ for 24 h before mixing. Suspension batches of 200 ml were prepared by immersing dried particles in silicon oil. The suspensions were mixed thoroughly with a stirrer for 2 h and stored in sealed containers. The fibre length distribution was not affected by mixing process. Fibre length distributions were determined from samples before and after the mixing process. Statistical analysis of variance resulted in no significant difference on level of confidence of 1% between the samples taken before and after the mixing process. Prior to measurement, the suspensions were stirred again for several minutes. Entrapped air was removed in vacuum before starting the rheological experiments.

Rheological measurements

Rheological measurements were carried out at a constant temperature of $25\text{ }^\circ\text{C}$ using a strain-controlled rheometer (Rheometric Scientific ARES, Orchestrator 6.5.1 software). A Couette geometry with a cup diameter of 34 mm, a bob diameter of 32 mm, and a bob length of

Table 1 Distribution parameters of the physical dimensions of glass filler particles (for fibres $r=0$, and for spheres $r=3$)

Physical dimension	Average $x_{r,10}$ (μm)	Average $x_{r,50}$ (μm)	Average $x_{r,90}$ (μm)
Fibre diameter	11.3	13.3	15.3
Fibre length	42.3	101.5	164.7
Sphere diameter	4.7	11.7	26.7

33.2 mm was used. It has to be noted that the influence of gap width on the rheological data was checked beforehand. Fibre/sphere suspensions were measured using Couette geometries with gap widths up to 5 mm. After correcting the apparent shear rate data based on a stepwise power law approximation as described in (Eischen and Windhab 2002), the viscosity functions collapsed well and no systematic shift of the curves could be detected.

For the determination of the time dependent flow behaviour, a constant shear rate was set and the independent variables were recorded as a function of time. Measurements were carried out in triplicate. For each run, a fresh sample was used.

Shear-rate dependent flow behaviour was determined by collecting the independent variables first at increasing and subsequently at decreasing shear rates. At each shear rate, the sample was allowed to equilibrate for 15 s and measurements were averaged during the succeeding 15 s. Before starting the rheological measurement, the suspensions were presheared at a shear rate of 0.5 s^{-1} and a preshear time of 2,000 s. Measurements were carried out in duplicate.

Determination of fibre orientation in flow

The evolution of fibre orientation distribution in mixed glass sphere and glass fibre suspensions was monitored using the RheoScope1 from Thermo Haake GmbH. The complete instrument (controlled stress rheometer, microscope, and CCD camera) is controlled by RheoWin software (Thermo Haake GmbH). Measurements were carried out at a constant temperature of $25 \text{ }^{\circ}\text{C}$ using a polished cone geometry with a diameter of 70 mm and a cone angle of 0.981° . For image acquisition, a lens with optic magnification of $10\times$ was used.

For the determination of the transient evolution of fibre orientation, a constant shear rate of 1 s^{-1} was set and the independent rheometric variables were recorded over time. Simultaneously with the rheological measurement, the image information was acquired for each data point. With respect to the evolution of rheological behaviour as a function of time, three time zones as indicated in Fig. 1 were determined, in which orientation angles of the fibres to the stream lines were assembled from five independent measurements. Image analysis was then performed on a Macintosh computer using the public domain software NIH Image.

The effect of shear history on the fibre angle distribution was evaluated by subjecting samples to step changes of shear rate ($0.2, 0.5, 1, 5,$ and 10 s^{-1}). Tests were performed in triplicate first at increasing and subsequently at decreasing shear rates with and without prior preshear treatment (0.5 s^{-1} for 600 s). For each step, a holding time of 90 s was allowed, resulting in 90

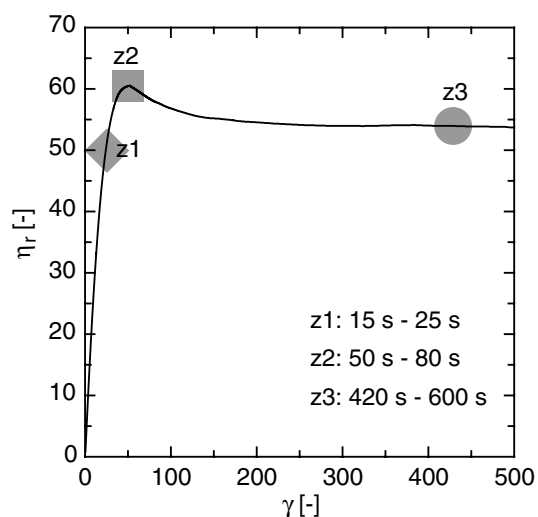


Fig. 1 Representation of the three time zones used for the determination of the fibre angle alignment evolution at constant shear rate

measurements and images per applied shear rate of which the second half was used for image analysis.

Results and discussion

Characterisation of the pure fibre and sphere suspensions

Before discussing the rheological behaviour of the mixed sphere/fibre suspensions, suspensions made up of individual shape classes shall be reviewed briefly. Viscosity as a function of solids volume concentration as well as time-dependent rheology will be discussed.

The results obtained for the viscosity measurements of suspensions of spheres and suspensions of fibres with the experimental conditions described in the previous section are presented in Fig. 2. A monotonic increase of the viscosities as the solids volume concentration, c_v , is increased can be seen for both suspension systems, with a strong increase as c_v approaches values around 0.6 and 0.4 for the sphere suspensions and the fibre suspensions, respectively. This is a classical behaviour (Metzner 1985).

A standard way to model the volume concentration dependence of the relative viscosity of non-colloidal suspensions is to use a semiempirical model such as Eq. 2. The best fit of our experimental relative upper Newtonian viscosities leads to the values of $c_{v, \text{max}} = 0.64$ and $k = 3.2$ for the suspensions of spheres, and $c_{v, \text{max}} = 0.43$ and $k = 4.2$ for the suspensions of fibres. Obtained values are in line with data reported in the literature for similar systems (Gonderet and Petit 1997; Metzner 1985). If suspensions of hard spheres are

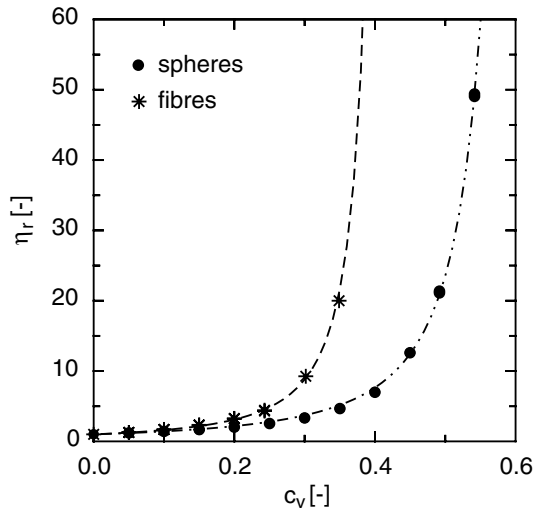


Fig. 2 Relative viscosities, η_r , of suspensions of spheres (filled circle) and fibres (asterisk) as a function of the total solids volume concentration, c_v high shear rate limit relative viscosities from measurements at decreasing shear rates for suspensions of glass spheres and glass fibres. Lines represent best fit values given by the Krieger–Dougherty equation (Eq. 2) with $c_{v, \max} = 0.64$ and $k = 3.2$ for spheres, and $c_{v, \max} = 0.43$ and $k = 4.2$ for fibres

ordered by flow the value of $c_{v, \max}$ can be larger and the value of k is usually smaller (Gonderet and Petit 1997). However, we will assume that the determined values are characteristic for the systems under investigation.

Figures 3 and 4 show the transient evolution of relative viscosity as a function of shear deformation for suspensions with a total solids volume concentration of $c_v = 0.2$ for pure fibres ($c_v = 0.2$, $c_{v, f} = 1.0$) and pure

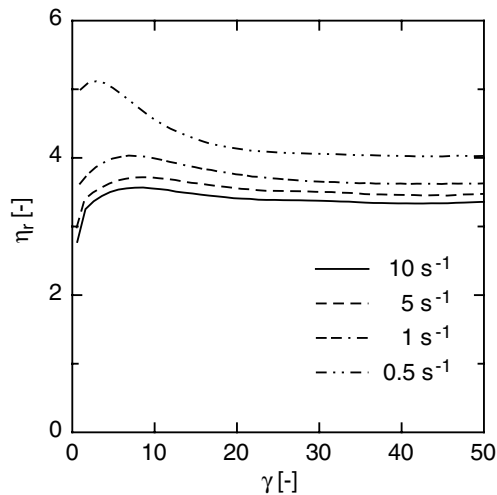


Fig. 3 Transient relative viscosities as a function of shear deformation for a glass fibre suspension with a solids volume concentration $c_v = 0.2$. Experimental results were obtained at four different shear rates ($\dot{\gamma} = 0.5, 1, 2, 5$, and 10 s^{-1})

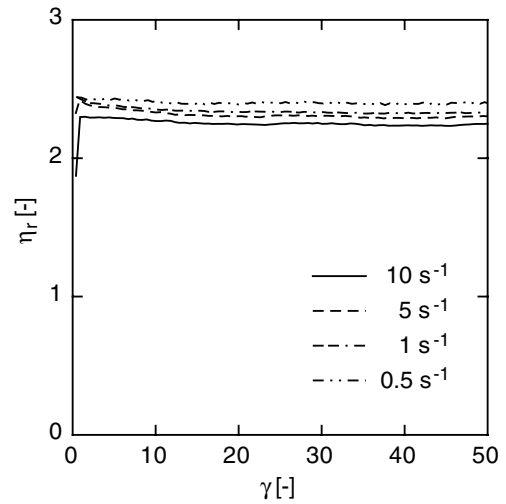


Fig. 4 Transient relative viscosities as a function of shear deformation for a glass sphere suspension with a solids volume concentration $c_v = 0.2$. Experimental results were obtained at four different shear rates ($\dot{\gamma} = 0.5, 1, 2, 5$, and 10 s^{-1})

spheres ($c_v = 0.2$, $c_{v, f} = 0.0$), respectively. Experiments were carried out with conditions described in the previous section and each displayed curve represents a measurement with a fresh sample.

The transient relative viscosity of the fibre suspensions as a function of shear deformation is characterised by a step rise at start-up of shear flow and a decrease of viscosity after reaching the maximum viscosity. For large deformations, the viscosity levels off to an equilibrium value. This behaviour is characteristic for non-dilute fibre suspensions (Barbosa et al. 1994). The rheopectic viscosity increase at the start up of shear flow can be attributed to a combination of following effects. (1) The formation of slip layers leads to very low start-up viscosity readings. (2) Fibre rotation is hindered through neighbouring fibres. The resulting stiffening of the fibre network leads to a viscosity increase. (3) Elastic properties in the fibre network caused by strong interactions leads to delayed response of the sheared material. In semi-dilute long fibre systems, increase in viscosity at small strains was found to be proportional on nL^3 , where L is the fibre length and n the number of fibres (Barbosa et al. 1994). Furthermore, the maximum viscosity was shown to depend only on total shear deformation and not on the contributions from shear rate and time, separately. This is also the case in our experiments within the shear rate range of $1\text{--}10 \text{ s}^{-1}$. Maximum viscosity as well as equilibrium viscosity appears at same shear deformation values independent of the applied shear rate. However, in the experiment where a shear rate of $\dot{\gamma} = 0.5 \text{ s}^{-1}$ was applied, maximum viscosity is shifted to lower deformations and equilibrium viscosity is only reached at larger deformations of

the sample material. In the second time segment of the curve, the viscosity decreases as a consequence of the orientation of the fibres on the shear plane. Equilibrium viscosity is reached when no further increase in average fibre orientation is reached through the flow.

The sphere suspensions show weak time dependent behaviour at a total solids volume concentration of $c_v=0.2$. Once the shear flow was switched on, the viscosity jumped to the equilibrium viscosity value. If solids volume concentration of the sphere suspensions is increased, some time dependency becomes apparent, as shown in Fig. 5. Thus, increasing concentration leads to increased interactions between the particles and some structure changes take place in flow. The thixotropy, however, is less pronounced than in the case of fibre suspensions.

Time-dependent flow behaviour of suspensions with mixtures of spheres and fibres

In this section, the time-dependent flow behaviour of suspensions with mixtures of fibres and spheres will be discussed with respect to fibre fraction and total solids volume concentration. The evolution of relative viscosity versus shear deformation from measurements with a constant shear rate of $\dot{\gamma} = 0.5 \text{ s}^{-1}$ which was well beyond the limit where wall slip was evident is shown in Fig. 6. Measurements were carried out using suspensions with a total solids volume concentration of $c_v=0.2, 0.3, 0.4$, and 0.5 . Within the given total c_v the volume concentration of fibres $c_{v, f}$ were varied from $0.0 \leq c_{v, f} \leq 1.0$. For example, a suspension with $c_v=0.2$ and $c_{v, f}=0.0$ contains only spheres while a suspension

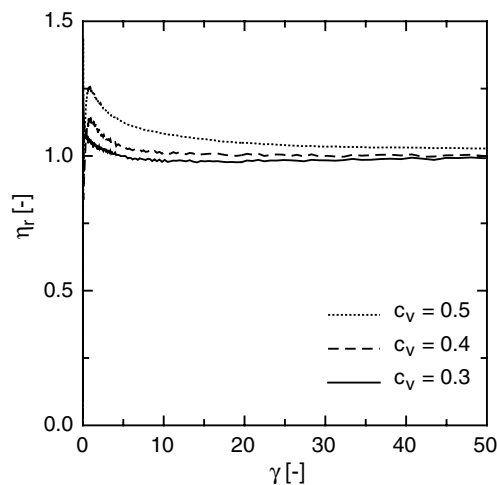


Fig. 5 Transient relative viscosities as a function of shear deformation for glass sphere suspensions with solids volume concentrations $c_v=0.3, 0.4$, and 0.5 . Experimental results were obtained at a shear rate of $\dot{\gamma} = 0.5, \text{ s}^{-1}$

with $c_v=0.2$ and $c_{v, f}=1.0$ is purely consists our of fibres. In the mixed case, e.g. for $c_v=0.2$ and $c_{v, f}=0.5$ half of the total solids volume concentration are fibres ($c_v=0.1$) and spheres ($c_v=0.1$). Before the samples were filled into the rheometer cup, they were thoroughly stirred to achieve as random as possible fibre orientation before the measurements. With increasing solids volume concentration, the maximum fibre fraction allowing for rheological measurements decreased from and $c_{v, f}=1.0$ ($c_v=0.2$) to 0.33 ($c_v=0.5$) as also indicates in Fig. 6. The use of higher fibre fractions resulted in highly viscous pastes and shear flow was dominated by wall slip.

In general, with increasing the total solids volume concentration and increasing fibre fraction more distinct time dependency can be observed, meaning that maximum viscosity values and deformation necessary to reach equilibrium viscosity increase. A rheopectic increase in viscosity in the low shear deformation regime can only be found for suspensions with a fibre volume concentration above a value of about $c_{v, f}=0.16$. After reaching the maximum viscosity value, these suspensions behave thixotropic over a long deformation range, which is much more pronounced than for pure fibre suspensions (see Fig. 3).

The most outstanding observation is the effect of fibre fraction on the equilibrium viscosity level. While for the suspensions with a total solids volume concentration of $c_v=0.2$ and 0.3 (Fig. 6a, b) the equilibrium viscosity is a monotonic increasing function of fibre fraction, this relationship changes at higher volume concentrations where increasing fibre fractions first lead to decreasing viscosity, and after passing a minimum at a fibre fraction of $c_{v, f}=0.167$ to increasing equilibrium viscosities at further increase of fibre fraction.

To evaluate whether the presence of spheres hindered the orientation of the fibres in the shear flow, experiments with the Rheoscope1 were carried out for suspensions with a total solids volume concentration of $c_v=0.5$ and fibre fractions from $c_{v, f}=0.125$ to 0.33 with experimental conditions as described in Materials and methods section. Figure 7 shows exemplary for the suspension with a fibre fraction of $c_{v, f}=0.33$ the evolution of fibre angle distribution from time zone 1 to zone 3 (see Fig. 1). An angle of 0° refers to a fully oriented fibre, whereas an angle of 90° refers to a fibre perpendicular to the direction of the flow.

For an ideally random fibre orientation, each orientation angle is equally possible. If the suspension is sheared fibres start to rotate and align parallel to the streamlines (Barbosa et al. 1994). Thus, with increasing shear deformation the fibre angle distribution is expected to shift from a flat curve without distinctive maximum to a curve with a maximum at small angles. This kind of behaviour could be observed in all performed measurements. No dependency of fibre fraction could be detected for the obtained results. This means

Fig. 6 Transient relative viscosities as a function of shear deformation for suspensions with mixture of spheres and fibres and solids volume concentrations $c_v = 0.2$ – 0.5 . Experimental results were obtained at a shear rate of $\dot{\gamma} = 0.5, \text{ s}^{-1}$

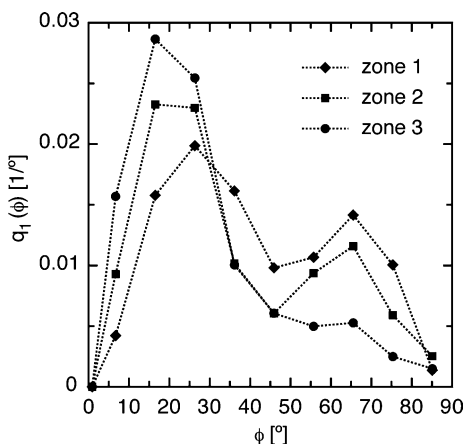
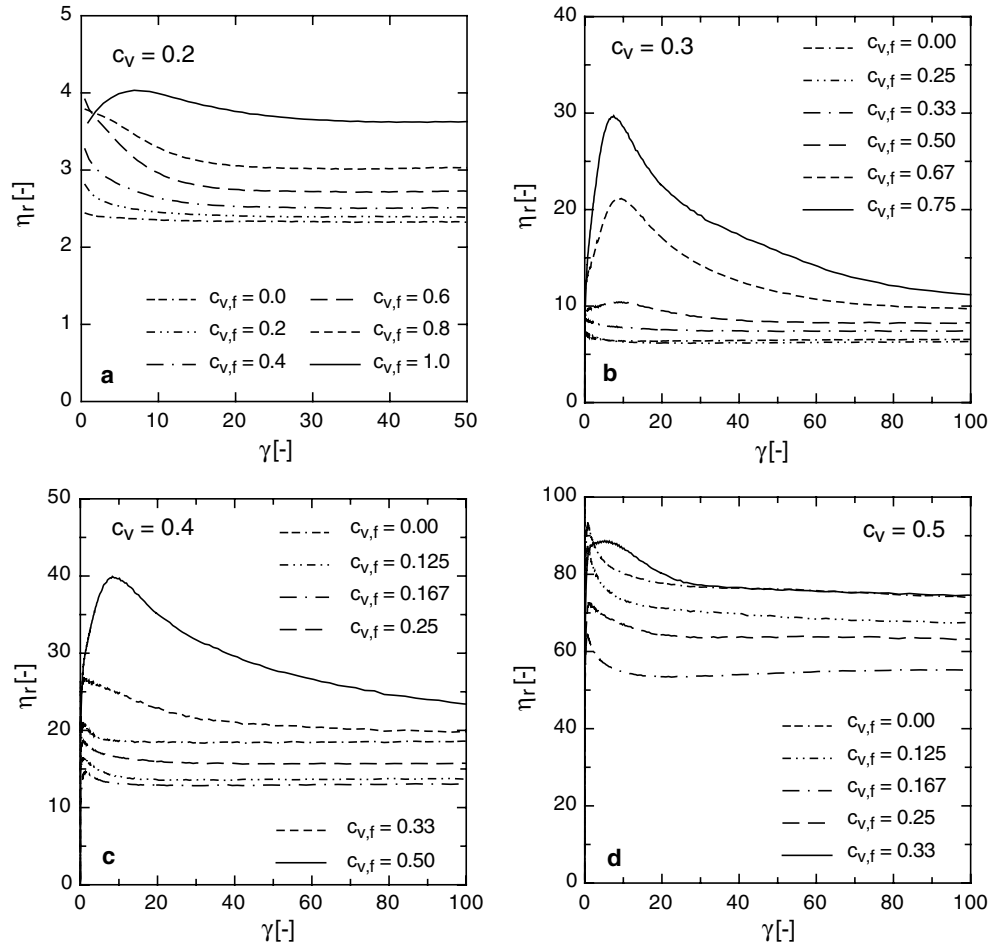


Fig. 7 Distribution of the orientation angles for a suspension with a solids volume concentration of $c_v = 0.5$ and a fibre fraction of $c_{v,f} = 0.33$ (corresponding to *solid line* in Fig. 6d). Transient measurements were obtained from image analysis performed with the Rheoscope 1 in time zones 1–3 according to Fig. 1

that fibre rotation and alignment is not affected by spherical particles in the suspension.

Shear-rate dependent flow behaviour of suspensions with mixtures of spheres and fibres

In the previous section, we demonstrated that for concentrated suspensions with a solids volume concentration of $c_v \leq 0.3$ the equilibrium relative viscosity at a shear rate of $\dot{\gamma} = 0.5 \text{ s}^{-1}$ is an increasing monotonic function of fibre fraction. For highly concentrated suspensions with mixtures of spheres and fibres and a solids volume concentration of $c_v \geq 0.4$ the minimum equilibrium relative viscosities were measured at a fibre fraction of around $c_{v,f} = 0.167$. However, the viscosity of concentrated suspensions is usually a function of shear rate and the slope in the shear thinning domain depends on concentration and on particle characteristics, such as size distribution and shape. Since measurements with a constant applied shear rate provide no information on the dependence on shear rate, results may be fragmentary, especially if the viscosity curves under

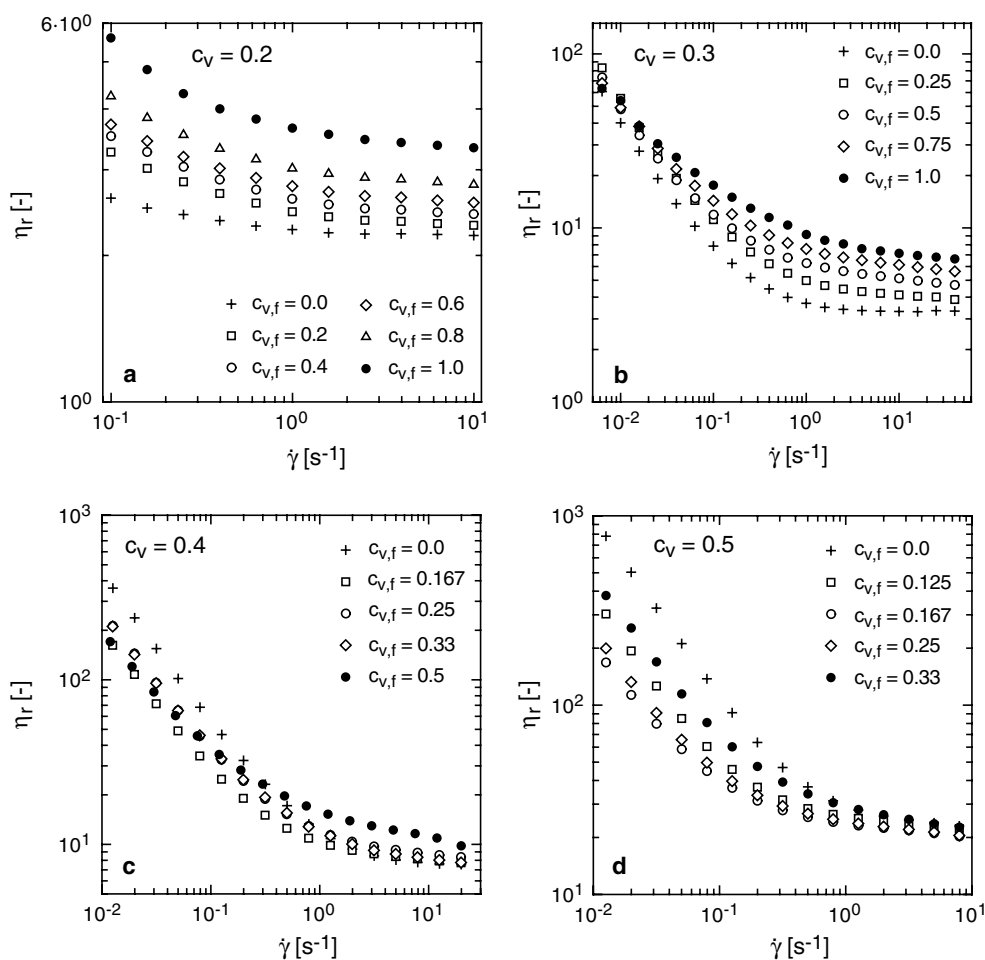
consideration intersect. The aim of this section is to provide detailed information about the shear rate dependent flow properties of suspensions with mixtures of spheres and fibres. Measurements with experimental conditions described in the Materials section have been performed with suspensions in a concentration range of $0.2 \leq c_v \leq 0.5$ and fibre fractions as used for the investigation of the transient flow behaviour. Figure 8 shows the relative viscosity as a function of shear rate for these suspensions. All data points represent measurements obtained at decreasing shear rates from presheared samples, meaning that fibres in the samples were oriented in shear flow prior to measurements.

With a solids volume concentration of $c_v = 0.2$, fibre fractions ranging from $0 \leq c_{v,f} \leq 1$ were used. The resulting viscosity curves are shown in Fig. 8a. They are characterised by shear thinning at low shear rates and an upper Newtonian viscosity plateau at a shear rate of around $\dot{\gamma} = 10 \text{ s}^{-1}$. The suspension of spheres ($c_{v,f} = 0$) exhibits least pronounced shear thinning and lowest viscosity. Both characteristics get more pronounced as the fibre fraction increases. Furthermore,

with increasing fibre fraction, the shear rate to reach the upper Newtonian viscosity plateau is slightly shifted to higher shear rates. If we raise the solids volume concentration to $c_v = 0.3$, similar characteristics for the shear-rate dependency of viscosity can be found (see Fig. 8b). Viscosity increases with increasing fibre fraction, particularly at higher shear rates. However, at a solids volume concentration of $c_v = 0.3$ the slope of the viscosity curve in the shear thinning regime is steeper for suspensions of spheres than for suspensions of fibres. As a consequence, the slopes of the viscosity versus shear rate curve decrease with increasing fibre fraction. At very low shear rates, the curves intersect. Thus, at the low shear rate limit, the suspension of fibres and the suspension of spheres have about the same viscosity; and for the mixed suspensions, the viscosity at the low shear rate limit decreases with increasing fibre fraction.

Further raising the total solids volume concentration to $c_v = 0.4$ and 0.5 leads to the shear-rate dependencies of the viscosity as depicted in Fig. 8c, d. The intersection of the curves shifts to higher shear rates. At a

Fig. 8 Relative viscosities as a function of shear rate for suspensions with mixture of spheres and fibres and solids volume concentrations of $c_v = 0.2$ – 0.5 . Experimental results were obtained at decreasing shear rates from presheared samples



concentration of $c_v=0.4$, the upper Newtonian viscosity of the suspension of spheres is still the lowest compared to the mixed suspensions, whereas in the case of solids volume concentration of $c_v=0.5$ the minimum upper Newtonian viscosity is obtained for the suspension with a fibre fraction $c_{v,f}=0.167$.

Measurements performed with the Rheoscope1 confirmed that the degree of fibre orientation was not the governing factor influencing the shear thinning behaviour of the investigated suspension systems. Figure 9 shows the evolution of the average fibre angle, $\phi_{50,0}$, as a function of the applied shear rate for suspensions with total solids volume concentration of $c_v=0.5$ and various fibres concentrations.

This representation was chosen because no influence of fibre fraction on the average orientation angle could be determined. Error bars indicate the standard deviation of the measured values. Standard deviation decreased with measurement time, indicating that at the start-up of the measurement, the average fibre angle depends on the initial fibre orientation in the sample, which in practice is not ideally random ($\phi_{50,0} \neq 45^\circ$). This effect gets balanced by applying preshear treatment before measurement. However, the chosen preshear treatment was not sufficient to fully orient the fibres. The average fibre angle is a decreasing function of shear rate for measurement performed at increasing shear rates for both, presheared samples (open squares) and samples without preshear treatment (filled squares). Steady values were reached for shear rates

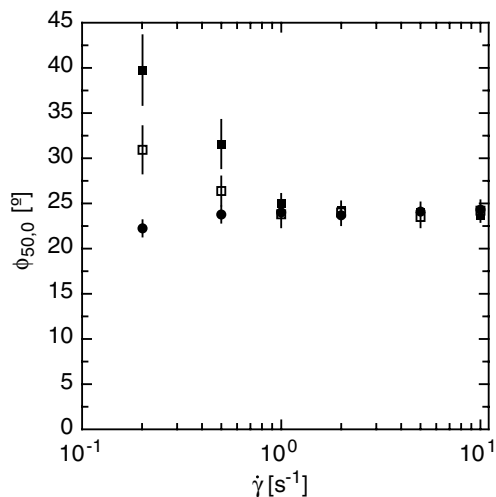


Fig. 9 Average fibre angle, $\phi_{50,0}$, as a function of shear rate for suspension with a solids volume concentration of $c_v=0.5$ and various fibre fractions. (*filled square*) Measurements at increasing shear rates without preshear treatment. (*open square*) Measurements at increasing shear rates with preshear treatment. (*filled circle*) Measurements at decreasing shear rates after up-ramp from presheared samples. *Error bars* indicate standard deviations of average values

$\dot{\gamma} \geq 2 s^{-1}$. At ensuing measurements performed at decreasing shear rates (filled circles), average fibre angle and its standard deviation remained roughly constant. Thus, the results show that spheres present in the system did not affect the degree of fibre orientation. As known for pure fibre suspensions (Barbosa et al. 1994) also in suspensions with mixtures of spheres and fibres as shown here, fibre orientation is predominantly a function of shear history.

Application of the Farris model to predict the high shear rate viscosity of suspensions with mixtures of fibres and spheres

In the previous section, the time-dependent and shear-rate dependent viscosities of suspensions made up with mixtures of fibres and spheres were characterised by rotational rheometry and image analysis. We showed that with increasing concentration, the dependency of fibre fraction on the relative high shear rate limit viscosity changes from a monotonically increasing behaviour to the occurrence of a minimum viscosity level at intermediate fibre fractions. Furthermore, image analysis showed that the degree of fibre orientation was not a function of fibre fraction for the investigated suspension systems.

The flow behaviour of suspensions with mixtures of fibres and spheres shows similarities to the properties of suspensions made up of fractions of fine and coarse particles of spherical shape where the coarse particles are suspended in a fluid made up of the suspension of fine spheres. The viscosity of such suspensions can be modelled using Eq. 3, and good agreement between measurement and model is usually found for suspensions where the size ratio of suspended particles is high (Farris 1968; Qin and Zaman 2003). In our case, the suspended particles belong to different shape classes. Based on the results from rheometry and in-line image analysis we can state that in shear flow, the fibres rotate freely in a suspension made up of spheres. Both, suspensions of spheres and suspensions of fibres were characterised with respect to their viscosity concentration relationships in the high shear rate regime. To recall, the diameter of the fibres corresponds with the diameter of the spheres, and the average fibre aspect ratio is 7.64.

Based on separate contributions from the suspensions of each shape class, the relative high shear rate limit viscosities of the mixed suspension systems were calculated using Eq. 3, adopting fibres as coarse particles. In Fig. 10 results calculated from Farris' model and rheological measurements are displayed as a function of fibre fraction for different solids volume concentrations. They show excellent qualitative and quantitative agreement between model and experiment.

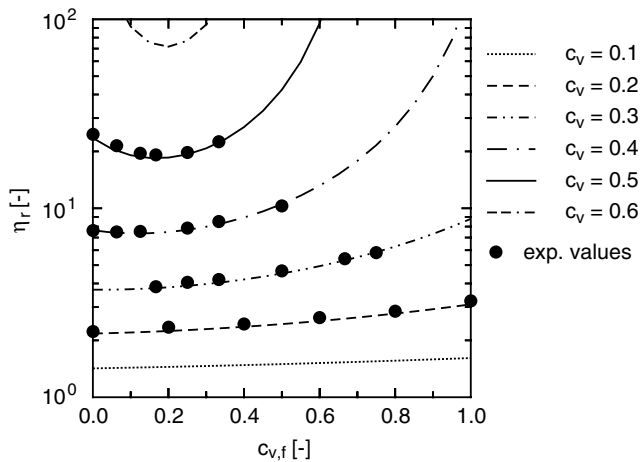


Fig. 10 Relative viscosities as a function of fibre fraction for suspensions with mixtures of spheres and fibres. *Lines* represent calculated values from Farris' model. (*filled circle*) Experimental results obtained at the high shear rate limit from suspensions at decreasing shear rates

Summary

In this paper, the flow behaviour of concentrated suspensions made up with mixtures of spheres and fibres was investigated using shear rheometry and in-line image analysis. Both time-dependent and shear-rate

dependent flow behaviour have been studied. Thereby solids volume concentration and fibre fraction of the suspensions were varied systematically. We found that, time dependency and shear rate dependency is a function of solids volume concentration and fibre fraction. At relatively low solids volume concentrations, the relative viscosity is a monotonic increasing function of the fibre fraction. Raising the solids volume concentration leads to a minimum viscosity measured for suspensions with intermediate fibre fractions. This minimum manifests in the low shear rate regime and shifts to higher shear rates with further increase of the solids volume concentrations.

Further it was demonstrated that the investigated suspension systems can be treated as suspensions of fibres dispersed in a fluid made up of the suspension of spheres. Based on the individual contribution from the suspensions of each shape class, the relative viscosities at the high shear rate limit were accurately fitted using the model proposed by Farris (1968) for mixtures of monodisperse spheres of different sizes. Thus, the results show the extended applicability of the Farris model for mixtures of particles from different shape classes.

Acknowledgements The authors gratefully acknowledge Thermo Haake GmbH, Karlsruhe/Germany for providing Rheoscope 1 to acquire data for in-line image analysis. Financial support by the Commission for Technology and Innovation CTI, Bern/Switzerland is acknowledged.

References

- Barbosa SE, Ercoli DR, Bibbó MA, Kenny JM (1994) Rheology of short-fibre composites: a systematic approach. *Compos Str* 27:83–91
- Barnes HA (1989) Shear-thickening (“dilatancy”) in suspensions of nonaggregating solid particles dispersed in Newtonian liquids. *J Rheol* 33:329–366
- Barnes HA (1997) Thixotropy—a review. *J Non-Newtonian Fluid Mech* 70:1–33
- Buscall R (1991) Effect of long-range repulsive forces on the viscosity of concentrated lattices: comparison of experimental data with an effective hard sphere model. *J Chem Soc Faraday Trans* 87:1365–1370
- Chang C, Powell RL (1994) Effect of particle size distribution on the rheology of concentrated bimodal suspensions. *J Rheol* 38:85–98
- Dabak T, Yucel O (1986) Shear viscosity behaviour of highly concentrated suspensions at low and high shear rates. *Rheol Acta* 25:527–533
- Einstein A (1906) Eine neue Bestimmung der Moleküldimensionen. *Ann Phys* 19:289–306
- Eischen J-C, Windhab EJ (2002) Viscosity of cocoa and chocolate products. *Appl Rheol* 12:32–34
- Farris RJ (1968) Prediction of the viscosity of multimodal suspensions from unimodal viscosity data. *Trans Soc Rheol* 12:281–301
- Frankel NA, Acrivos A (1967) On the viscosity of a concentrated suspension of solid spheres. *Chem Eng Sci* 22:847–853
- Frith WJ, Mewis J, Strivens TA (1987) Rheology of concentrated suspensions: experimental investigations. *Powder Technol* 51:27–34
- Ganani E, Powell RL (1985) Suspensions of rodlike particles—literature review and data correlations. *J Compos Mater* 19:194–215
- Gonderet P, Petit L (1997) Dynamic viscosity of macroscopic suspensions of bimodal sized solid spheres. *J Rheol* 41:1261–1274
- Krieger IM (1972) Rheology of monodisperse lattices. *Adv Colloid Int Sci* 3:111–136
- Krieger IM, Dougherty TJ (1959) A mechanism for non-Newtonian flow in suspensions of rigid spheres. *Trans Soc Rheol* 3:137–152
- Metzner AB (1985) Rheology of suspensions in polymeric liquids. *J Rheol* 29:739–775
- Mewis J (1979) Thixotropy—a general review. *J Non-Newtonian Fluid Mech* 6:1–20
- Mewis J, Macosco CW (1993) Suspension rheology. In: Macosco CW (ed) *Rheology: principles, measurements and applications*. VCH Publishers, New York, pp 425–474
- Mooney M (1951) The viscosity of a concentrated suspension of spherical particles. *J Colloid Sci* 6:162–170
- Petrich MP, Koch DL, Cohen C (2000) An experimental determination of the stress-microstructure relationship in semi-concentrated fiber suspensions. *J Non-Newtonian Fluid Mech* 95:101–133
- Petrie CJS (1999) The rheology of fibre suspensions. *J Non-Newtonian Fluid Mech* 87:369–402

-
- Probstein RF, Sengun MZ, Tseng T-C (1994) Bimodal model of concentrated suspension viscosity for distributed particle sizes. *J Rheol* 38:811–829
- Qin K, Zaman AA (2003) Viscosity of concentrated colloidal suspensions: comparison of bidisperse models. *J Colloid Int Sci* 266:461–467
- Schmidt M, Münstedt H (2002) Rheological behaviour of concentrated monodisperse suspensions as a function of preshear conditions and temperature: an experimental study. *Rheol Acta* 41:193–204
- Stover CA, Koch DL, Cohen C (1992) Observation of fibre orientation in simple shear flow of semi-dilute suspensions. *J Fluid Mech* 238:277–296
- Sudduth RD (1993) A new method to predict the maximum packing fraction and the viscosity of solutions with a size distribution of suspended particles. *J Appl Polym Sci* 48:37–55
- Tsai SC, Botts D, Plouff J (1992) Effects of particle properties on the rheology of concentrated noncolloidal suspensions. *J Rheol* 36:1291–1304
- Villagran FV, McCabe GM, Wong VYL (1996) Process for making reduced fat nut spreads US Patent 5,490,999. Procter & Gamble Co, Cincinnati, OH, USA
- Windhab EJ (2000) Fluid immobilization—a structure-related key mechanism for the viscous behavior of concentrated suspension systems. *Appl Rheol* 10:134–139